International Journal of Heat and Mass Transfer 214 (2023) 124435

Contents lists available at ScienceDirect

International Journal of Heat and Mass Transfer

journal homepage: www.elsevier.com/locate/ijhmt

Transient thermal management characteristics of a porous fin with radially outwards fluid flow

Muhammad M. Abbas, Mohsen Torabi, Ankur Jain*

Mechanical and Aerospace Engineering Department, University of Texas at Arlington, 500W First St, Rm 211, Arlington, TX 76019, USA

ARTICLE INFO

Article history:
Received 11 April 2023
Revised 26 May 2023
Accepted 19 June 2023

Keywords:
Fins
Porous medium
Transient thermal transport
Fin effectiveness
Thermal Management
Energy Storage

ABSTRACT

Thermal management and energy storage problems often utilize extended surfaces, also known as fins for enhanced heat transfer. While thermal conduction is usually the dominant mode of heat transfer in a solid fin, the use of porous fins that include advective thermal transport due to porous fluid flow has also been investigated. In particular, the steady state thermal performance of a porous fin with pressure-driven radially outwards flow has been studied. While such results are helpful for studying problems that are inherently steady state in nature, such results do not readily apply to problems where heat removal or energy storage occurs only over a short period of time. This work presents transient thermal analysis of a porous fin with radial porous fluid flow driven by a pressure gradient. It is shown that the transient temperature field in the fin is governed by a transient convection-diffusion-reaction (CDR) equation, the solution for which is derived in the form of Bessel functions. Based on this solution, the evolution of fin performance with time is examined. Comparison of heat removed by the porous fin with a baseline case without any fin is carried out. The time taken to reach steady state is calculated. Key non-dimensional parameters appearing in this problem are identified and their impact on fin performance over time is investigated. Since fin porosity improves advective thermal transport but suppresses diffusive transport at different rates at different times, therefore, it is shown that for a given operating time, there may exist an optimal porosity that maximizes the rate of heat removal. It is shown that the operating time period of the fin plays a key role in determining whether fin porosity strongly impacts heat removal rate or not. Consequently, it is shown that it is important to consider transient effects in determining whether the use of a porous fin is beneficial at all, and, if so, what is the optimal fin porosity to use. This work contributes towards porous fin theory, and offers practical design guidelines for improving and optimizing the transient performance of porous fins.

1. Introduction

Heat transfer enhancement through extended surfaces, also referred to as fins is a well-studied topic in heat transfer with a long research history [1,2]. One of the first analysis of extended surface heat transfer was presented more than a century ago [3]. Fundamentally, a fin offers increased surface area for heat transfer, which, under well-designed conditions results in greater heat removal rate than without the fin [1]. Fins are used universally, with heat transfer enhancement in heat exchanger tubes [4] and cooling of semiconductor chips [5] being two representative examples. In addition to thermal management, the use of fins has also been widely investigated for improving latent energy storage by improving the rate at which heat is transferred into a bed of phase change material [6]

A large body of literature already exists on the use of analytical methods to determine the temperature distribution in a fin towards improving and optimizing fin performance. In general, the principle of energy conservation is used to model heat transfer in a fin while accounting for factors such as fin shape [7] and flow conditions around the fin [8]. Doing so results in differential equations of varying complexity [1,2], based on which, the temperature distribution, and thus, various fin performance parameters such as fin effectiveness and fin efficiency can be derived [9]. Similar literature is also available in the field of fin-based enhancement of latent energy storage, wherein optimization of fin shape and size has been carried out to maximize energy delivered by the fin into a bed of phase change material [6]. The use of entropy minimization techniques [10,11] and constructal design [12] to optimize fin design can also be found in the literature. While such optimization has typically been limited to fins of manufacturable shapes, topology optimization of fins has also attracted much recent attention, due to the ability to print structures of arbitrary shapes

* Corresponding author.
E-mail address: jaina@uta.edu (A. Jain).

https://doi.org/10.1016/j.ijheatmasstransfer.2023.124435
0017-9310/

Nomenclature

R_0	fin base radius (m)
$\bar{A}$	Péclet number
$\bar{B}$	ratio of convective heat removal and diffusion terms
Bi_{tip}	Biot number at the fin tip
c_f	fluid heat capacity ($Jkg^{-1}K^{-1}$)
c_s	solid heat capacity ($Jkg^{-1}K^{-1}$)
h	convective heat transfer coefficient around the fin ($Wm^{-2}K^{-1}$)
h_{tip}	convective heat transfer coefficient at the fin tip ($Wm^{-2}K^{-1}$)
k_{eff}	effective thermal conductivity ($Wm^{-1}K^{-1}$)
k_f	fluid thermal conductivity ($Wm^{-1}K^{-1}$)
k_s	solid thermal conductivity ($Wm^{-1}K^{-1}$)
L	fin radial length (m)
$\bar{L}$	non-dimensional fin radial length
r	radial coordinate (m)
t	time (s)
T	temperature (m)
T_∞	ambient temperature around the fin (K)
$T_{\infty,tip}$	ambient temperature at the fin tip (K)
T_b	fin base temperature (K)
U	velocity (m)
w	fin height (m)
$\bar{w}$	non-dimensional fin height
Δp	pressure difference (Pa)
K	permeability (m^2)
μ	viscosity ($kgm^{-1}s^{-1}$)
ξ	non-dimensional radial coordinate
ϕ	porosity
ρ_f	fluid density (kgm^{-3})
ρ_s	solid density (kgm^{-3})
θ	non-dimensional temperature
$\theta_{\infty,tip}$	non-dimensional fin tip temperature
τ	time (s)

using additive manufacturing. Analysis is available for a number of non-standard fin shapes such as tree-like [13], fractal fins [14], gradient fins [15] and irregularly-shaped topology optimized fins [16]. While the modeling of conduction and convection usually results in linear equations, other complications, such as temperature-dependent [17] or spatially-varying [18] thermal properties and radiation [19] introduce non-linearities into the problem, making it more difficult to solve.

Most of the literature on theoretical heat transfer analysis in fins addresses non-porous fins, in which, conduction is the only heat transfer mechanism available within the fin. A relatively smaller body of literature has addressed thermal transport in porous fins. In most such cases, buoyancy-driven cross-flow of a fluid is assumed to permeate the fin, resulting in additional heat removal from the fin [20]. The governing equation in such a case has been shown to be non-linear [21], and a number of analytical [22–24] and numerical [20,21,25] techniques have been used to determine and optimize fin performance. Porous fin performance under local thermal non-equilibrium conditions [26] and in natural convection conditions [27,28] has been analyzed. The effect of radiation [29], temperature-dependent properties [30] and heat generation [31] in porous fins has been accounted for. Porous fin performance has been compared with solid fins [32,33]. In addition, recently, steady-state thermal analysis of a porous fin with radially outwards porous fluid flow, driven by a radial pressure gradient has been reported [33]. A key advantage of this porous fin configuration is that the porous flow is pressure-driven, resulting in greater flow speed and thus greater advective heat removal than buoyancy-driven flow. Advective heat removal in such a fin may complement or even exceed the underlying conductive heat transfer [33]. A porous fin effectiveness has been defined for characterizing thermal performance of such a porous fin compared to an equivalent non-porous fin [33]. In such a case, the porosity of the fin becomes an important design choice due to its opposite effects on conductive and advective heat removal mechanisms.

While most of the past theoretical heat transfer analysis for fins has addressed steady-state performance, in certain scenarios, transient performance of the fin may also be important. For example, semiconductor chip thermal management is a highly transient process [34], depending on how power dissipation on the chip varies over time. Often, a large amount of heat needs to be dissipated in a short period, followed by a period of inactivity. Similarly, several energy storage problems occur over a limited time duration, governed by how long the heat source is available [6]. To analyze and optimize such problems, it is important to comprehensively understand how fin heat transfer evolves with time prior to reaching steady state. Unfortunately, commonly available steady-state models are not sufficient to address this important need. Instead, the transient governing energy equations must be written and solved. Specifically, in the case of a porous fin with radially outwards flow, while recent work has presented steady-state thermal analysis [33], transient performance of the porous fin is not yet fully understood. Important questions related to transient performance include the time taken to reach steady state, and how fin performance parameters such as fin effectiveness evolve before steady state is reached. From a design perspective, it is of interest to determine whether an optimal fin porosity exists that may maximize total heat removal over a given short period of time prior to reaching steady state. Towards this, an analytical approach is much more desirable than numerical simulations, due to the fundamental insights offered by analytical solutions, such as the identification of important non-dimensional parameters.

This work presents theoretical analysis of transient heat transfer performance of a porous fin, in which, a pressure gradient drives radially outwards porous flow. An exact solution for the fin temperature distribution based on Bessel functions of non-zero order is derived. Expressions for fin effectiveness, as well as porous fin performance relative to an equivalent non-porous fin, both as functions of time are derived. The time taken to reach steady state is analyzed. It is shown that under certain conditions, there exists an optimal fin porosity that maximizes total heat removal over a given operating time period. Below a threshold time period, however, the use of a porous fin is not beneficial. The dependence of these key metrics on various non-dimensional parameters of the problem is analyzed. Results presented here contribute towards an improved understanding of a novel class of porous fins, with possible applications in both energy storage and thermal management.

2. Problem definition

Consider the transient thermal transport problem associated with heat removal from a hot, constant temperature surface by a porous fin. This problem is defined in cylindrical coordinates, in which, a radial fin of constant thickness removes heat from a hot, annular cylinder, as shown in the schematic presented in Fig. 1(a). In addition to conventional conductive heat removal through the fin, its porous nature additionally enables advective heat removal due to radially outwards porous flow through the fin. Such a flow could be driven by, for example, a pressure gradient between fluid inside the cylinder and the tip of the fin. Other flow mechanisms such as electro-osmotic flow may also be possible, but are not explicitly considered here. Both conductive and advective heat removal mechanisms are closely related to the fin porosity, since

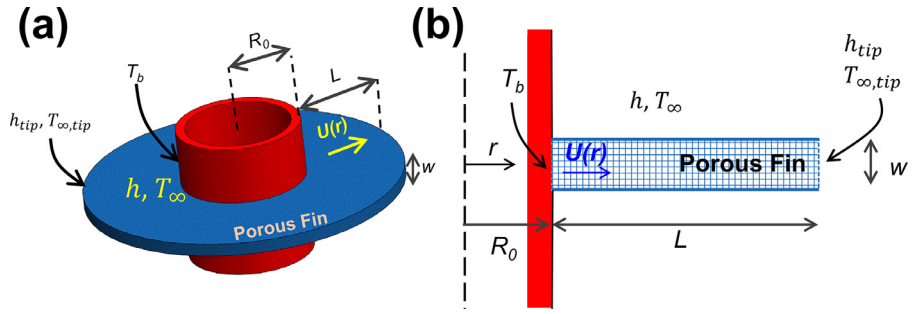

Fig. 1. (a) Schematic and (b) Cross-section of a porous fin with pressure gradient driven radially outwards flow through the fin that provides an additional mechanism for heat removal from the fin base.

porosity affects both effective thermal conductivity that drives conductive heat removal, as well as the radially outwards flow field that drives advective heat removal.

While a previous work has analyzed this problem in steady state [33], there are several practical applications where heat transfer by the fin occurs only over a limited time. An example includes thermal management of a semiconductor chip or a Li-ion battery, where, in both cases, heat generation occurs only for a relatively short period of time, during which, the fin may not reach steady state. As another example, fin-based enhancement of latent energy storage in a phase change material (PCM) around a hot source is also a transient process, depending on how long the hot source, such as solar heat, is available. It is important to develop a transient thermal model to predict porous fin performance as a function of time, since previously developed steady state models do not address this need.

A schematic of the porous fin is shown in Fig. 1(a), along with a cross-section view in Fig. 1(b). A transverse radial fin is attached to the outer surface of a hot hollow cylinder of radius R_0. The outer radius and width of the fin are $R_0 + L$ and w, respectively. The fin base is assumed to remain at a fixed temperature T_0. The fin is composed of a porous material and sealed on the top and bottom surfaces, so that a pressure gradient driven radially outwards fluid flow from the base of the fin, $r = R_0$ to its tip $r = R_0 + L$ is established. Along the length of the fin, heat loss to the surroundings occurs through convective heat transfer, represented by a convective heat transfer coefficient h along with freestream temperature T_∞. For generality, separate values of convective heat transfer coefficient h_{tip} and freestream temperature $T_{\infty,tip}$ are assumed at the fin tip. Thermal conductivity, heat capacity and density are denoted by k, c and ρ, respectively, with subscripts s and f for the solid and fluid components of the fin, respectively. Porosity and permeability of the fin material are denoted by ϕ and K, respectively. The entire fin is assumed to be initially at a temperature T_∞. For a given time period, the interest is in determining the heat removed by the fin through both conductive and advective mechanisms, and to develop an understanding of how to design the fin, for example, how to choose the fin porosity in order to maximize heat removal over a given time period. Such a performance evaluation of the fin first requires determining the transient temperature field in the fin.

A number of assumptions are made in order to carry out this analysis. The fin is assumed to be axisymmetric, which is usually the case in most practical problems. All thermal and flow properties, as well as those associated with the porous material, such as porosity and permeability are assumed to be uniform and independent of temperature. This is a reasonable assumption when the change in temperature is small enough for variation in properties to be negligible [35]. The thermal field is assumed to evolve over time in a steady flow field, which is also a standard assumption in convective heat transfer analysis [36]. Finally, consistent with standard porous flow analysis, the flow field is assumed to be laminar and Darcian, which is reasonable for flows at relatively low velocity [37]. As a result, an expression for the steady velocity field may be derived as follows [33,37]

$$U(r) = \frac{\mathrm{K} \cdot \Delta p}{\mu \cdot \ln\left(\frac{R_0+L}{R_0}\right) \cdot r} \tag{1}$$

Note that the $1/r$ dependence of the velocity field helps conserve mass.

Based on the assumptions listed above, the temperature field in the porous is spatially one-dimensional, in the radial direction only. The general energy conservation equation that governs the transient temperature field $T(r,t)$ may be written as

$$\frac{k_{eff}}{r}\frac{\partial}{\partial r}\left(r\frac{\partial T}{\partial r}\right) - \frac{\phi\rho_f c_f}{r}\frac{\partial}{\partial r}(r \cdot T \cdot U(r)) - \frac{h}{w}(T - T_\infty) = (\rho c)_{eff}\frac{\partial T}{\partial t} \tag{2}$$

Where $(\rho c)_{eff} = [\phi\rho_f c_f + (1-\phi)\rho_s c_s]$ and the three terms on the left hand side represent diffusion, advection and convective heat removal, respectively, in an infinitesimal fin element. The boundary conditions and initial condition for the temperature field are

$$T = T_b \quad (r = R_0) \tag{3}$$

$$-k_{eff}\frac{\partial T}{\partial r} = h_{tip}\left(T - T_{\infty,tip}\right) \quad (r = R_0 + L) \tag{4}$$

$$T = T_\infty \quad (t = 0) \tag{5}$$

where k_{eff} is the effective thermal conductivity of the porous medium. In general, k_{eff} may be obtained based on an appropriate average of the solid and fluid thermal conductivities, in which, the porosity plays a key role. A commonly used weighted average based on porosity, i.e., $k_{eff} = \phi k_f + (1-\phi)k_s$ [37] is adopted in this work.

In order to simplify this problem and to ensure the generality of the solution derived, it is cast in non-dimensional form using the following variables and parameters:

$$\xi = \frac{r}{R_0};\ \tau = \frac{k_{eff}t}{(\rho c)_{eff}R_0^2};\ \theta = \frac{T - T_\infty}{T_b - T_\infty};\ \bar{A} = \frac{\mathrm{K} \cdot \rho_f c_f \cdot \Delta p \cdot \phi}{\mu \cdot \ln\left(\frac{R_0+L}{R_0}\right) k_{eff}};$$
$$\bar{B} = \frac{hR_0^2}{k_{eff}w};\ \bar{L} = \frac{L}{R_0};\ Bi_{tip} = \frac{h_{tip}R_0}{k_{eff}};\ \theta_{\infty,tip} = \frac{T_{\infty,tip} - T_\infty}{T_b - T_\infty} \tag{6}$$

Here, ξ and τ are the non-dimensional spatial and time coordinates, respectively. θ is the non-dimensional temperature. Bi_{tip} and $\theta_{\infty,tip}$ are the Biot number and non-dimensional tip temperature that represent the convective boundary condition at the tip. $\bar{L}$ is the non-dimensional fin length. $\bar{A}$ and $\bar{B}$ are non-dimensional parameters that represent the rates of advective heat transfer

through the fin and convective heat loss from the fin surface, respectively, both expressed relative to the rate of conductive heat transfer. Note that the fin width w appears within $\bar{B}$.

This results in the following non-dimensional transient energy conservation equation

$$\frac{1}{\xi}\frac{\partial}{\partial\xi}\left(\xi\frac{\partial\theta}{\partial\xi}\right)-\frac{\bar{A}}{\xi}\frac{\partial\theta}{\partial\xi}-\bar{B}\theta=\frac{\partial\theta}{\partial\tau} \tag{7}$$

Eq. (7) represents a transient Convection-Diffusion-Reaction (CDR) equation [38–40]. The non-dimensional temperature field is also subject to the following boundary conditions and initial condition

$$\theta=1 \quad (\xi=1) \tag{8}$$

$$-\frac{\partial\theta}{\partial\xi}=Bi_{tip}\left(\theta-\theta_{\infty,tip}\right) \quad \left(\xi=1+\bar{L}\right) \tag{9}$$

$$\theta=0 \quad (\tau=0) \tag{10}$$

3. Solution of the problem

Due to the non-homogeneity appearing in the boundary condition given by Eq. (8), one may first substitute $\theta(\xi,\tau)=v(\xi)+u(\xi,\tau)$, where v and u are the steady state and transient components, respectively, of the temperature distribution. By inserting this form of θ in the governing equation and boundary conditions, one may write the following differential equation for $v(\xi)$:

$$\frac{1}{\xi}\frac{d}{d\xi}\left(\xi\frac{dv}{d\xi}\right)-\frac{\bar{A}}{\xi}\frac{dv}{d\xi}-\bar{B}v=0 \tag{11}$$

subject to the following boundary conditions:

$$v=1 \quad (\xi=1) \tag{12}$$

$$-\frac{dv}{d\xi}=Bi_{tip}\left(v-\theta_{\infty,tip}\right) \quad \left(\xi=1+\bar{L}\right) \tag{13}$$

The $v(\xi)$ problem is indeed the steady-state problem for the porous fin with radially outwards flow, which has been solved in a recent paper [33]. The solution for the problem is given by [33]

$$v(\xi)=\xi^{\bar{A}/2}\left[c_1 I_{\bar{A}/2}\left(\sqrt{\bar{B}}\xi\right)+c_2 K_{\bar{A}/2}\left(\sqrt{\bar{B}}\xi\right)\right] \tag{14}$$

where the coefficients c_1 and c_2 are obtained on the basis of the boundary conditions. I and K are modified Bessel functions of the first and second kind, respectively [41]. Expressions for c_1 and c_2 are available from the recent steady-state analysis [33] and are not reproduced here for brevity.

The differential equation governing the rest of the temperature field, $u(\xi,\tau)$ is given by

$$\frac{1}{\xi}\frac{\partial}{\partial\xi}\left(\xi\frac{\partial u}{\partial\xi}\right)-\frac{\bar{A}}{\xi}\frac{\partial u}{\partial\xi}-\bar{B}u=\frac{\partial u}{\partial\tau} \tag{15}$$

subject to

$$u=0 \quad (\xi=1) \tag{16}$$

$$-\frac{\partial u}{\partial\xi}=Bi_{tip}\cdot u \quad \left(\xi=1+\bar{L}\right) \tag{17}$$

$$u(\xi,\tau)=-v(\xi) \quad (\tau=0) \tag{18}$$

Note that the $u(\xi,\tau)$ problem is free of non-homogeneities in the governing equation as well as the boundary conditions. Therefore, a solution may be derived using the method of separation of variables. Substituting $u(\xi,\tau)=\xi^{\frac{\bar{A}}{2}}\cdot f(\xi)\cdot g(\tau)$ and separating the equations for $f(\xi)$ and $g(\tau)$, one may derive the following form of the solution

$$u(\xi,\tau)=\sum_{m=1}^{\infty}\xi^{\frac{\bar{A}}{2}}\cdot s_m\left(J_{\frac{\bar{A}}{2}}(\omega_m\xi)+c_{2,m}\cdot Y_{\frac{\bar{A}}{2}}(\omega_m\xi)\right)e^{-\lambda_m^2\tau} \tag{19}$$

where $\omega_m=\sqrt{\lambda_m^2-\bar{B}}$, and J and Y are Bessel functions of the first and second kind, respectively. The order of both Bessel functions that appear in the solution is $\bar{A}/2$. The eigenvalues λ_m and coefficient $c_{2,m}$ may be determined by applying boundary conditions given by Eqs. (16) and (17). Rearrangement of the resulting equations may be shown to result in the following eigenequation:

$$\begin{aligned}&\left(\sqrt{\lambda^2-\bar{B}}\,Y_{\frac{\bar{A}}{2}-1}\left[\left(1+\bar{L}\right)\sqrt{\lambda^2-\bar{B}}\right]+Bi_{tip}\cdot Y_{\frac{\bar{A}}{2}}\left[\left(1+\bar{L}\right)\sqrt{\lambda^2-\bar{B}}\right]\right)\\&J_{\frac{\bar{A}}{2}}\left[\sqrt{\lambda^2-\bar{B}}\right]-\left(\sqrt{\lambda^2-\bar{B}}\,J_{\frac{\bar{A}}{2}-1}\left[\left(1+\bar{L}\right)\sqrt{\lambda^2-\bar{B}}\right]\right.\\&\left.+Bi_{tip}\cdot J_{\frac{\bar{A}}{2}}\left[\left(1+\bar{L}\right)\sqrt{\lambda^2-\bar{B}}\right]\right)Y_{\frac{\bar{A}}{2}}\left[\sqrt{\lambda^2-\bar{B}}\right]=0\end{aligned} \tag{20}$$

further, it can be found from Eq. (16) that $c_{2,m}=-\frac{J_{\frac{\bar{A}}{2}}(\omega_m)}{Y_{\frac{\bar{A}}{2}}(\omega_m)}$. Therefore, the solution for $u(\xi,\tau)$ may be written as

$$u(\xi,\tau)=\sum_{m=1}^{\infty}\xi^{\frac{\bar{A}}{2}}\cdot s_m\left(J_{\frac{\bar{A}}{2}}(\omega_m\xi)-\frac{J_{\frac{\bar{A}}{2}}(\omega_m)}{Y_{\frac{\bar{A}}{2}}(\omega_m)}\cdot Y_{\frac{\bar{A}}{2}}(\omega_m\xi)\right)e^{-\lambda_m^2\tau} \tag{21}$$

The last remaining set of coefficients, s_m may be determined by using the initial condition given by Eq. (18) in conjunction with the principle of orthogonality of the eigenfunctions. Note that due to the appearance of the advective term in the governing equation, the principle of orthogonality differs slightly from that for pure-diffusion problems. Specifically, as shown in prior work on a CDR problem [42], a weighing function $\xi^{1-\frac{\bar{A}}{2}}$ must be included in the expression for orthogonality of eigenfunctions. Eq. (18) is inserted into (19), followed by multiplying both sides by $\xi^{1-\frac{\bar{A}}{2}}\left(J_{\frac{\bar{A}}{2}}(\omega_{m'}\xi)+c_{2,m'}\cdot Y_{\frac{\bar{A}}{2}}(\omega_{m'}\xi)\right)$ and integrating from $\xi=1$ to $\xi=1+\bar{L}$. Based on orthogonality, this results in elimination of all terms except one, a formal proof for which is available in the literature [42]. This leads to the following expression for s_m

$$s_m=-\frac{\int_1^{1+\bar{L}}v_m(\xi)\left(J_{\frac{\bar{A}}{2}}(\omega_m\xi)+c_{2,m}Y_{\frac{\bar{A}}{2}}(\omega_m\xi)\right)\xi^{1-\frac{\bar{A}}{2}}\,d\xi}{\int_1^{1+\bar{L}}\xi\left(J_{\frac{\bar{A}}{2}}(\omega_m\xi)+c_{2,m}Y_{\frac{\bar{A}}{2}}(\omega_m\xi)\right)^2 d\xi} \tag{22}$$

Note that the denominator in Eq. (22) is the norm of the eigenfunctions of this problem.

This completes the derivation of the solution of the problem. The final solution for the temperature distribution on the fin is given by Eqs. (14) and (21), along with Eqs. (20) and (22).

Based on the temperature distribution derived here, one may write the following expression for the dimensional rate of heat removal from the fin base as a function of time

$$q(t)=\left(-k_{eff}\left(\frac{\partial T}{\partial r}\right)_{r=R_0}+\phi\rho_f c_f\cdot \mathrm{U}(R_0)(T_b-T_\infty)\right)2\pi R_0 w \tag{23}$$

Note that the first and second terms in the expression for $q(t)$ represent conductive and advective rates of heat removal, respectively.

Based on the instantaneous rate of heat removal derived above, the following expression for the non-dimensional heat removal rate may be written

$$\begin{aligned}\bar{q}(\tau) &= \frac{q(t)}{k_{eff}(T_b - T_\infty)2\pi w} \\ &= \bar{A} - \sqrt{\bar{B}}\left(c_1 I_{\frac{\bar{A}}{2}-1}\left(\sqrt{\bar{B}}\right) - c_2 K_{\frac{\bar{A}}{2}-1}\left(\sqrt{\bar{B}}\right)\right) \\ &\quad - \sum_{m=1}^{\infty} s_m \omega_m \left(J_{\frac{\bar{A}}{2}-1}(\omega_m) - \frac{J_{\frac{\bar{A}}{2}}(\omega_m)}{Y_{\frac{\bar{A}}{2}}(\omega_m)} \cdot Y_{\frac{\bar{A}}{2}-1}(\omega_m)\right) e^{-\lambda_m^2 \tau} \quad (24)\end{aligned}$$

While Eq. (24) represents the instantaneous rate of heat removal at any given time, an averaged rate of heat removal up to a given time may be of practical interest for applications in which a finite amount of time is available for heat transfer. One may derive

$$\begin{aligned}\bar{q}_{avg}(\tau) = \frac{\int_0^t q(t^*)dt^*}{t} &= \bar{A} - \sqrt{\bar{B}}\left(c_1 I_{\frac{\bar{A}}{2}-1}\left(\sqrt{\bar{B}}\right) - c_2 K_{\frac{\bar{A}}{2}-1}\left(\sqrt{\bar{B}}\right)\right) \\ &\quad - \sum_{m=1}^{\infty} s_m \omega_m \left(J_{\frac{\bar{A}}{2}-1}(\omega_m) - \frac{J_{\frac{\bar{A}}{2}}(\omega_m)}{Y_{\frac{\bar{A}}{2}}(\omega_m)} \cdot Y_{\frac{\bar{A}}{2}-1}(\omega_m)\right) \\ &\quad \frac{1 - e^{-\lambda_m^2 \tau}}{\lambda_m^2 \tau} \quad (25)\end{aligned}$$

4. Fin transient performance parameters

One may define the fin effectiveness to be the ratio of heat removal rate by the fin and heat rate that would be removed directly from the base in the absence of the fin

$$\eta(t) = \frac{\left(-k_{eff}\left(\frac{\partial T}{\partial r}\right)_{r=R_0} + \phi \rho_f c_f \cdot \mathrm{U}(R_0)(T_b - T_\infty)\right)2\pi R_0 w}{2\pi R_0 w h (T_b - T_\infty)} \quad (26)$$

which can be shown to result in

$$\begin{aligned}\eta(\tau) = \frac{1}{Bi}\Bigg[&\bar{A} - \sqrt{\bar{B}}\left(c_1 I_{\frac{\bar{A}}{2}-1}\left(\sqrt{\bar{B}}\right) - c_2 K_{\frac{\bar{A}}{2}-1}\left(\sqrt{\bar{B}}\right)\right) \\ &- \sum_{m=1}^{\infty} s_m \omega_m \left(J_{\frac{\bar{A}}{2}-1}(\omega_m) - \frac{J_{\frac{\bar{A}}{2}}(\omega_m)}{Y_{\frac{\bar{A}}{2}}(\omega_m)} \cdot Y_{\frac{\bar{A}}{2}-1}(\omega_m)\right) e^{-\lambda_m^2 \tau}\Bigg] \quad (27)\end{aligned}$$

Note that the fin effectiveness is a function of time, since the heat removal rate by the fin changes over time. It is expected that the fin effectiveness will be very high at early times, owing to large conductive heat removal due to large temperature gradient between the base and the fin.

In addition, it is also of interest to define a fin effectiveness on the basis of comparison of porous fin performance with a non-porous fin of the same geometry and operating under identical conditions. Such a comparison is pertinent in order to understand whether a porous fin offers improved thermal performance than its non-porous equivalent. While porosity in the fin offers advective heat removal that is absent from the non-porous fin, yet, the porous fin has lower effective thermal conductivity, implying that its conductive heat removal may be lower than the non-porous fin. Therefore, it is important to compare the total heat removal by both porous and non-porous fins. This may be done by defining the porous fin effectiveness as the ratio of heat removal by the two fins. Similar to fin effectiveness, the porous fin effectiveness is also a function of time as follows:

$$\eta_{porous}(\tau) = \frac{k_{eff}}{k_s} \frac{\bar{A} - \sqrt{\bar{B}}\left(c_1 I_{\frac{\bar{A}}{2}-1}\left(\sqrt{\bar{B}}\right) - c_2 K_{\frac{\bar{A}}{2}-1}\left(\sqrt{\bar{B}}\right)\right) - \sum_{m=1}^{\infty} s_m \omega_m \left(J_{\frac{\bar{A}}{2}-1}(\omega_m) - \frac{J_{\frac{\bar{A}}{2}}(\omega_m)}{Y_{\frac{\bar{A}}{2}}(\omega_m)} \cdot Y_{\frac{\bar{A}}{2}-1}(\omega_m)\right) e^{-\lambda_m^2 \tau}}{-\sqrt{\bar{B}_s}\left(c_{1,s} I_1\left(\sqrt{\bar{B}_s}\right) - c_{2,s} K_1\left(\sqrt{\bar{B}_s}\right)\right) + \sum_{m=1}^{\infty} s_{m,s} \omega_{m,s}\left(J_1(\omega_{m,s}) - \frac{J_0(\omega_{m,s})}{Y_0(\omega_{m,s})} \cdot Y_1(\omega_{m,s})\right) e^{-\lambda_{m,s}^2 \tau}} \quad (28)$$

where, in the denominator, $\omega_{m,s} = \sqrt{\lambda_{m,s}^2 - \bar{B}_s}$, $\bar{B}_s = \frac{hR_0^2}{k_s w}$ and $\lambda_{m,s}$ are obtained from roots of the eigenequation given by Eq. (20) while using $\bar{B}_s$ instead of $\bar{B}$ and $\bar{A} = 0$ in order to model the non-porous fin.

5. Results and discussion

In order to highlight key features of this transient thermal problem, the transient temperature field in the fin is determined first, followed by computation of heat removal and other performance parameters of the fin. In each case, the transient behavior of fin performance is of particular interest.

5.1. Number of terms needed

Firstly, due to the infinite series nature of the transient temperature distribution derived in this work, it is important to determine the number of eigenvalues that must be accounted for in computations. This helps determine a reasonable balance between accuracy and computational time. In general, the greater the number of eigenvalues considered, the more accurate is the computed temperature, but at a greater computational cost. This is because, in principle, the series solution is exact only if an infinite number of eigenvalues have been considered. However, each additional eigenvalue adds to the computational cost, not only to compute the additional term, but also to compute the eigenvalue itself by determining the next root of the eigenequation, given, in this case, by Eq. (20). Once converged, increasing the number of terms further offers only a negligible improvement in accuracy while continuing to increase computational cost. Therefore, it is of interest to determine the minimum number of terms needed for a specific computation. In the present case, temperature distribution along the fin is computed at two specific times, while including different number of eigenvalues, denoted by N. Results are presented in Fig. 2, which shows that the computed temperature distribution with $N = 5$ and $N = 10$ terms are practically identical at both times. Therefore, the use of five terms is found to be sufficient at the two times considered in Fig. 2. Since the number of terms needed for convergence of an eigenfunction-based series solution usually increases at smaller times, therefore, in the present case, all results are presented with a conservative value of $N = 50$. It is found that the increase in computational cost between $N = 10$ and $N = 50$ is not significant, and, therefore, $N = 50$ is a reasonable choice.

5.2. Typical transient temperature distribution

For a fixed set of problem parameters $\bar{A} = 1.0$, $\bar{B} = 2.0$, $\bar{L} = 2.0$, $Bi_{tip} = 0.5$, $\theta_{tip,\infty} = 0.0$, Fig. 3(a) plots temperature distributions in the fin at different times. This is supplemented by plots of temperature at different fin locations as functions of time in Fig. 3(b). These plots show that thermal transport into the fin causes temperature rise over time, first in regions next to the fin base and slowly encompassing the entire fin. As time passes, a balance is reached between advective/conductive thermal transport into the fin and convective heat removal into the ambient, resulting in steady state. For example, at $\tau = 0.005$, only the region up to $\xi = 1.30$ has heated up significantly, while the rest of the fin is still nearly at the initial temperature. As time passes, the temperature curve shifts rightwards and upwards, indicating deeper and

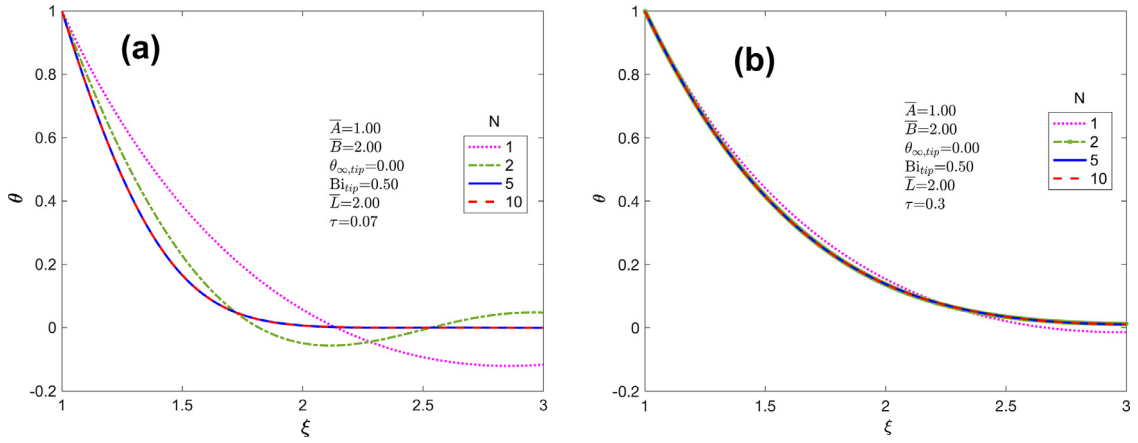

Fig. 2. Effect of number of eigenvalues considered in the analytical solution: Temperature distribution along the fin at (a) $\tau = 0.07$, (b) $\tau = 0.30$. Curves corresponding to different number of eigenvalues are presented. Parameter values are $\bar{A} = 1.0$, $\bar{B} = 1.0$, $\bar{L} = 2.0$, $Bi_{tip} = 0.5$, $\theta_{\infty,tip}$=0.0.

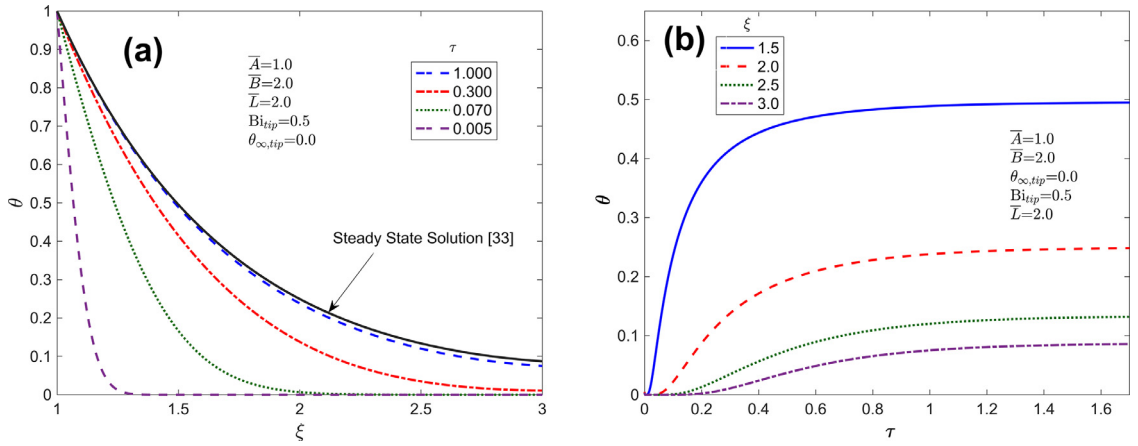

Fig. 3. Typical fin temperature field: (a) Fin temperature distribution along the fin at multiple times. (b) Fin temperature at multiple locations as functions of time. Parameter values are $\bar{A} = 1.0$, $\bar{B} = 1.0$, $\bar{L} = 2.0$, $Bi_{tip} = 0.5$, $\theta_{\infty,tip}$=0.0. The steady state solution is also shown in (a) for reference.

deeper penetration of heat into the fin. At large times, the transient temperature field computed using the model presented here approaches the independently computed steady state profile [33], also shown in Fig. 3(a).

It is notable that as time passes, there is a reduction in the slope of the temperature curve at the fin base, which represents the conductive rate of heat removal, per Eq. (24), indicating reduction in conductive heat removal over time. Temperature curves as functions of time presented in Fig. 3(b) show that, depending on how far a point is from the fin base, there is an initial period of negligible temperature rise before temperature begins to rise appreciably. This is mainly due to the time taken for thermal transport from its base to a given fin location. As expected, the closer a point is to the fin base, the shorter is this initial period, the earlier is steady state reached, and, finally, the greater is the temperature rise at steady state.

5.3. Impact of advective ($\bar{A}$) and convective ($\bar{B}$) thermal transport

The two key transport-related non-dimensional parameters that appear in the transient porous fin problem are $\bar{A}$ and $\bar{B}$, which represent advective thermal transport down the fin and convective heat removal from the fin, respectively, both expressed relative to the rate of conduction heat transfer down the fin. The impact of $\bar{A}$ and $\bar{B}$ on the transient temperature field in the fin is examined first, with particular interest in the time taken to reach steady state. Such analysis helps understand the effect of changing various input parameters that make up the non-dimensional parameters $\bar{A}$ and $\bar{B}$. For example, the effect of changing the pressure drop Δp or fin width w on fin performance can be understood by analyzing the impact of changing $\bar{A}$ or $\bar{B}$, respectively.

The transient fin temperature distribution is computed using Eqs. (14) and (22) for several values of $\bar{A}$. All other parameters are held constant as follows: $\bar{B} = 2.0$, $\bar{L} = 2.0$, $Bi_{tip} = 0.5$ and $\theta_{\infty,tip} = 0.0$. Since steady state is reached only asymptotically at infinite time, therefore, the time taken for the temperature to reach 95% of the eventual temperature at very large time, denoted by τ_{95} is taken to represent the time to reach steady state. Results are plotted in Fig. 4, where Fig. 4(a) plots the tip temperature as a function of time for each case and Fig. 4(b) plots τ_{95} as a function of $\bar{A}$ at multiple locations on the fin. Several key features of the transient temperature distribution in this problem are evident from Figs. 4(a) and (b). First of all, there is a small initial time during which there is no significant temperature rise at the fin tip. This is because of the finite time taken for thermal energy to reach the fin tip due to advection and conduction from the hot base. Following this initial period, temperature rises rapidly, and then slows down as the fin approaches steady state. Fig. 4(a) shows greater temperature rise for larger values of $\bar{A}$, which is expected because $\bar{A}$ represents advective transport of heat. Therefore, the larger the value of $\bar{A}$, the more rapidly does the point of interest heat up. In addition to the magnitude of temperature, $\bar{A}$ also influences the speed at which the fin approaches steady state. This is best observed in Fig. 4(b), where the time taken to reach steady state, τ_{95} is found

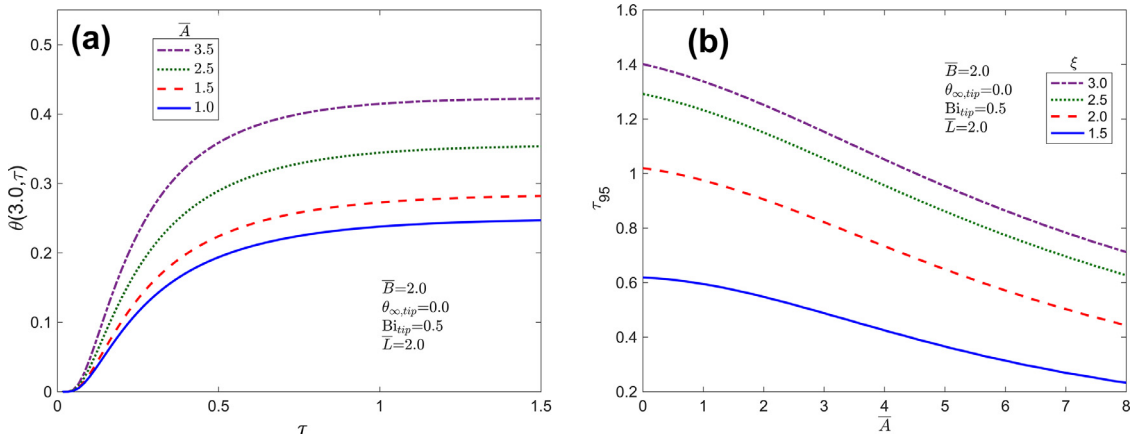

Fig. 4. Effect of $\bar{A}$: (a) Fin temperature at tip as a function of time for multiple values of $\bar{A}$, (b) Time required for 95% of temperature change up to steady state as a function of $\bar{A}$ at multiple fin locations. Other parameter values are $\bar{B} = 1.0$, $\bar{L} = 2.0$, $Bi_{tip} = 0.5$, $\theta_{\infty,tip} = 0.0$.

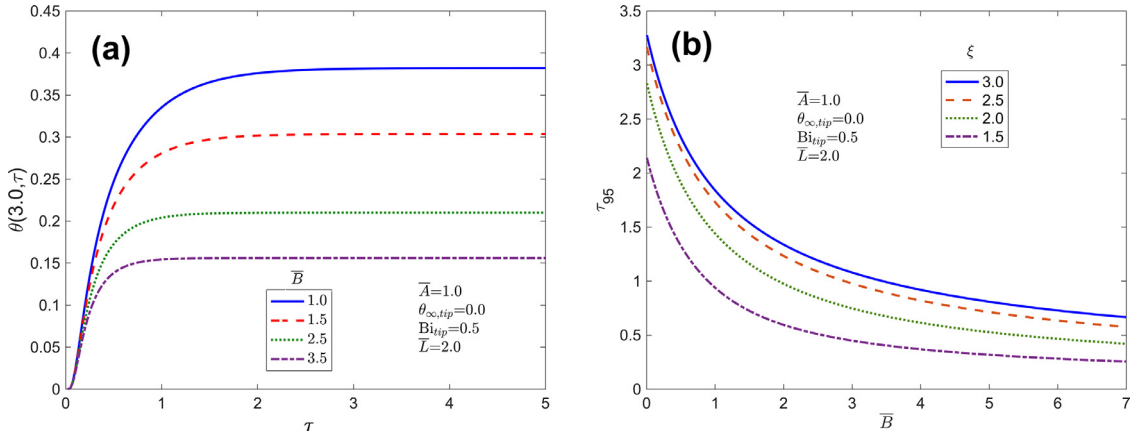

Fig. 5. Effect of $\bar{B}$: (a) Fin temperature at tip as a function of time for multiple values of $\bar{B}$, (b) Time required for 95% of temperature change up to steady state as a function of $\bar{B}$ at multiple fin locations. Other parameter values are $\bar{A} = 1.0$, $\bar{L} = 2.0$, $Bi_{tip} = 0.5$, $\theta_{\infty,tip} = 0.0$.

to decrease with increasing $\bar{A}$. Finally, Fig. 4(b) also shows that different locations at the fin take different times to reach steady state. The closer a point is to the base, the faster it reaches steady state due to rapid thermal transport from the base to the point. Depending on the value of $\bar{A}$, the time to reach steady state at the fin tip may be more than 40–50% greater than the time to reach steady state at the mid-point of the fin.

A similar analysis of the impact of $\bar{B}$ on the transient temperature field is presented in Fig. 5. Temperature at the tip of the fin is plotted as a function of time for multiple values of $\bar{B}$ in Fig. 5(a), and the time taken to reach steady state is plotted as a function of $\bar{B}$ for multiple locations on the fin in Fig. 5(b). A few aspects of the effect of $\bar{B}$ on the transient temperature field are similar to the effect of $\bar{A}$ – there is an initial period of slow temperature rise, followed by prolonged, rapid temperature rise, eventually leading asymptotically to steady state. Unlike $\bar{A}$, the larger the value of $\bar{B}$, the lower is the temperature rise. This is because $\bar{B}$ represents the rate at which the fin convectively loses heat to the surrounding medium. A larger value of $\bar{B}$ implies greater heat loss, and, therefore, lower temperature rise. It is found that $\bar{B}$ also has a significant impact on the time taken to reach steady state. At any given location, a large value of $\bar{B}$ results in faster arrival of steady state. This is because large $\bar{B}$ implies greater convective heat removal that counteracts the conductive/advective heat flow from the fin base, resulting in reaching steady state faster.

Note that changes in $\bar{B}$ may be brought about by changes in any of the parameters that appear in the definition of $\bar{B}$, including the convective heat transfer coefficient, fin inner radius, effective thermal conductivity and fin width. Therefore, the plots shown in Fig. 5 represent the impact of changing any one or more of these parameters on the transient thermal response of the porous fin. For example, curves at decreasing values of $\bar{B}$ shown in Fig. 5 represent the impact of increasing the fin thickness.

Further, note that the range of non-dimensional time τ considered in this work is around 2.0. Assuming porous steel fin of inner radius 5 cm with water as the fluid and porosity of 0.5, this translates to a dimensional time of up to 653 s. This indicates that under these conditions, the analysis presented above may be relevant to cooling problems that last a few hundreds of seconds, for example, the discharge process of the Li-ion cell that generates heat over a period of 600 s at a C-rate of 6C. In case the fluid is air instead of water, the range of dimensional time for the same range of τ is much lower, which may be relevant for the problem of cooling of a microprocessor chip, in which, the heat load changes with a time period of few tens of milliseconds or lower. A key advantage of non-dimensional analysis carried out here is that multiple disparate applications such as the two listed above can be analyzed within a single framework.

5.4. Heat removal rates as functions of time

The previous sub-section focuses mainly on fin temperature distribution and the time taken to reach steady state. In addition, it is also of much interest to examine how the rate of heat removal

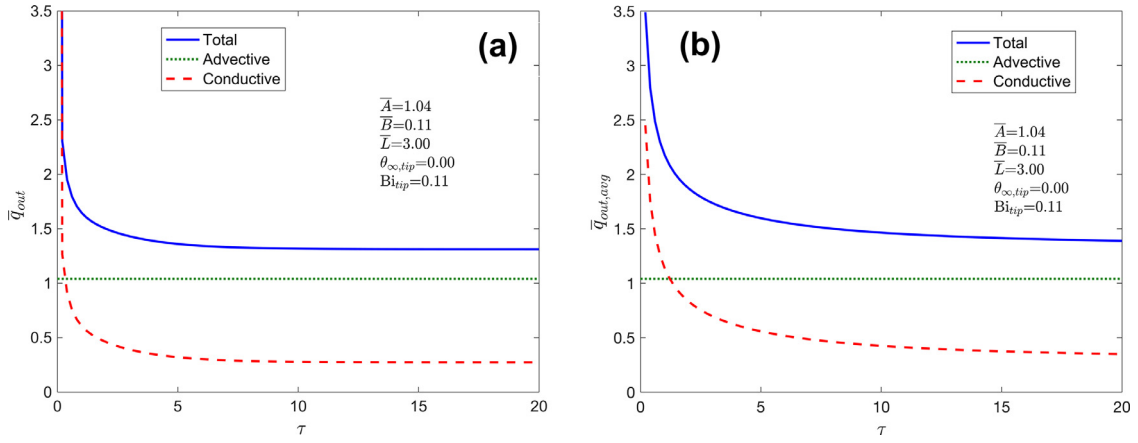

Fig. 6. Advective, conductive and total heat removal rates through the fin as functions of time: (a) and (b) present instantaneous and averaged heat removal rates. Parameter values are $\bar{A} = 1.04$, $\bar{B} = 0.11$, $\bar{L} = 3.0$, , $Bi_{tip} = 0.11$, $\theta_{\infty,tip}$=0.00.

by the fin varies with time. While steady state heat removal by the porous fin has been characterized in the past [33], there are several scenarios, as outlined in Section 1, where only a finite amount of time is available for the heat removal process, during which, the fin may not even reach steady state. In such scenarios, steady state performance of the porous fin is not relevant, and, instead, it is important to understand how heat removal by the fin changes with time prior to reaching steady state. For a fixed set of problem parameters ($\bar{A} = 1.04$, $\bar{B} = 0.11$, $\bar{L} = 3.0$, $Bi_{tip} = 0.11$, $\theta_{\infty,tip} = 0.0$), Fig. 6 plots the non-dimensional fin heat removal rate as a function of time. In order to facilitate a fundamental understanding of this problem, both advective and conductive rates of heat removal, as defined by Eq. (24) are also plotted, in addition to the total heat removal rate. Fig. 6(a) plots the instantaneous rates of heat removal, per Eq. (24), whereas the average rate of heat removal up to a certain time, which may be of greater practical importance, is plotted as a function of time in Fig. 6(b). Since the advective rate of heat removal is simply equal to $\bar{A}$, per Eq. (24), therefore, the advective curves in Figs. 6(a) and 6(b) are both horizontal straight lines, corresponding to the value of $\bar{A} = 1.04$ used here. In contrast, the conductive rate of heat removal depends strongly on time. At early times, when there is a large temperature gradient between the fin base and the rest of the fin, there is very large conductive heat removal, per Eq. (24). As the fin heats up, this temperature difference reduces, and the conductive rate of heat removal drops sharply, eventually reaching a steady value. Trends similar to the instantaneous heat removal rates shown in Fig. 6(a) are also found in the average heat removal rates plotted in Fig. 6(b). The reduction in conductive rate of heat removal over time seen in Figs. 6(a) and (b) are consistent with Fig. 3(a), where the slope of the temperature field at the fin base, $(\frac{\partial\theta}{\partial\xi})_{\xi=1}$ is found to reduce and reach a steady value as time increases.

The plots in Fig. 6 show that heat removal at early times is dominated by the conductive mechanism, whereas, there is a certain time at which the two mechanisms have equal contributions (around $\tau = 1.2$, as shown in Fig. 6(b)), and at later times, advective heat removal dominates. This shifting away of the dominating mechanism from conductive to advective over time is an important consideration in the design of practical systems when there is only finite time available for heat removal. In such cases, the time available for heat removal must be compared against the transition time shown in Fig. 6, based on which, one must design to either enhance advective or conductive heat removal mechanism by changing underlying parameters such as the porosity of the fin or the applied pressure difference. For example, if the total time available is relatively small, then one must maximize conductive heat transport by choosing a low value of porosity, or not using a porous fin at all. In contrast, if the time available for heat transfer is much larger than the conduction-to-advection transition time, then it may be beneficial to improve advective heat removal by increasing fin porosity.

5.5. Effect of porosity on fin performance

Porosity is a key parameter in the design of the porous fin. The porosity of the fin material can be easily varied, and must be carefully chosen in order to maximize the desired objective, which, in most cases, is the total heat removed by the fin. Introducing porosity into the fin may impact advective and conductive heat removal mechanisms in opposite directions. For example, greater porosity facilitates greater advective heat removal through increased porous flow down the fin. Mathematically, this occurs due to greater advective component of heat removal given by Eq. (24), with increasing ϕ. On the other hand, increasing the fin porosity reduces effective thermal conductivity, which reduces conductive heat removal. Due to these opposing effects, it is of interest to determine if the total heat removed increases or decreases with increasing porosity, or, if there is an optimal value of the porosity that maximizes total heat removed. Past analysis [33] showed that, in steady state, an optimal value of the fin porosity exists under certain conditions, whereas under other conditions, making the fin porous may not be beneficial at all. It is of interest to extend such analysis to transient conditions, in order to facilitate the design of porous fins for scenarios with limited time available for heat transfer.

In order to analyze this problem over a transient time period, the total heat removed as well as its conductive and advective components are plotted as functions of fin porosity in Fig. 7. Plots are presented at four different times. Values of parameters are chosen to be consistent with past steady state analysis [33]. In short, baseline solid and fluid materials are taken to be aluminum and air, with constant properties corresponding to room temperature. Additionally, $K = 5.7 \times 10^{-9}$ m^2, $R_0 = 5$ cm, $L = 15$ cm, $w = 5$ cm, $\Delta p = 100$ Pa, $h = 50$ Wm^{-2}K^{-1}. These plots use Eqs. (14), (21) and (23). Results indicate that at early times, heat removal is dominated by conductive thermal transport, which is due to the large temperature gradient in the fin at small times. As time passes and the fin gets hotter, the temperature gradient reduces, and, therefore, the rate of conductive heat removal reduces sharply. In contrast, the rate of advective heat removal remains invariant with time. As a result of this, it is found that at early times, using a fin with large porosity actually reduces total heat removal, as evidenced by the monotonically reducing plot for the total heat re-

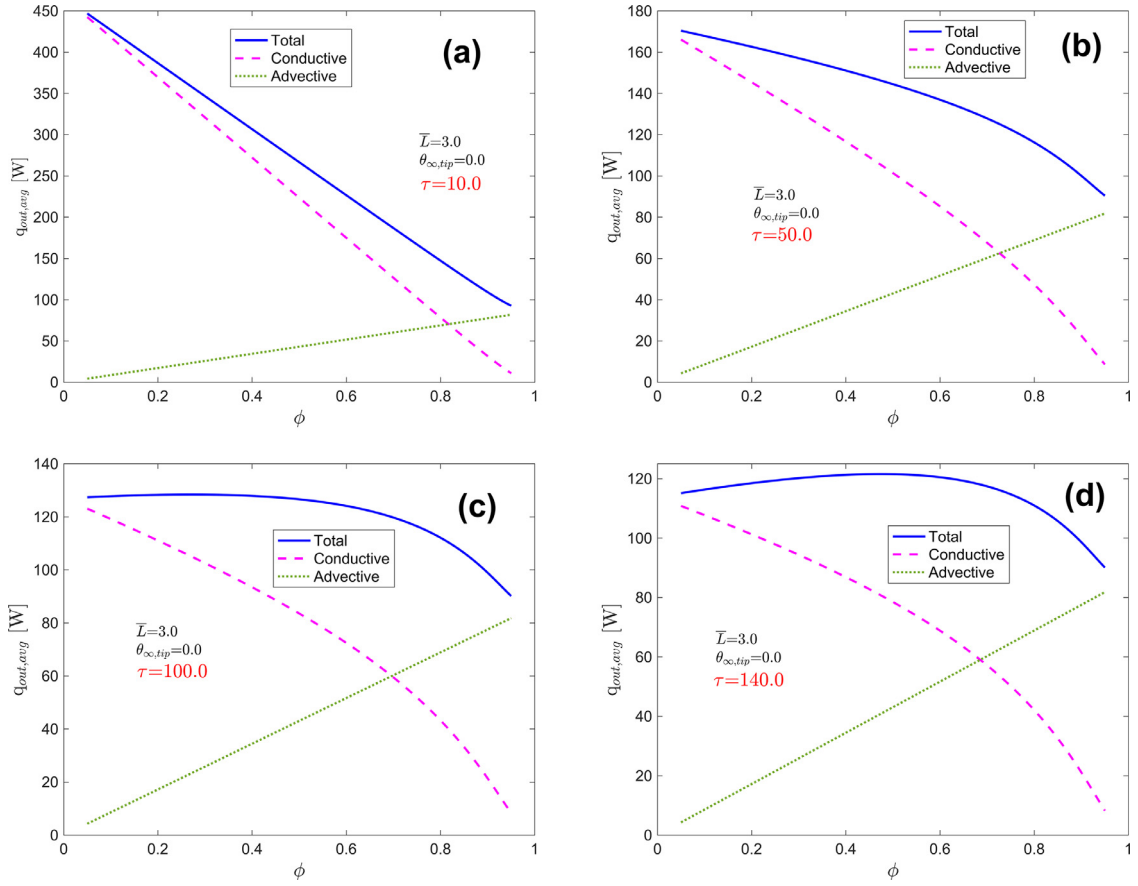

Fig. 7. Impact of porosity: Averaged heat removal rates as well as conductive and advective components as functions of porosity up to (a) $\tau = 10.0$, (b) $\tau = 50.0$, (c) $\tau = 100.0$ and (a) $\tau = 140.0$. Parameter values are $\bar{L} = 3.0$, $\theta_{\infty,tip} = 0.0$. Values of other fin parameters are given in Section 5.4.

moval in Figs. 7(a) and (b). This occurs because large porosity results in reduced effective thermal conductivity, and thus a reduction in conductive heat removal, which is the dominant heat removal mechanism at small times. As time passes, the total heat removal curve is found to become more and more curved, as seen in Fig. 7(c), and eventually become non-monotonic by developing a maxima at a certain value of porosity, as seen in Fig. 7(d). This indicates that if the fin operates for a sufficiently long time, there exists an optimal value of the porosity at which the total heat removal is maximized.

The optimal porosity of the fin, ϕ_{opt}, is computed and plotted in Fig. 8 as a function of the maximum time period available for heat removal, τ_{max} for the same set of parameters as the previous Figure. Fig. 8 shows an optimal value of zero porosity for short time periods, due to early dominance of conductive heat removal, which is exacerbated by porosity in the fin. Beyond a certain time, conductive heat removal has diminished significantly, such that making the fin porous is now favorable. This period in Fig. 8 is characterized by a very sharp rise in the value of ϕ_{opt}, followed by saturation at large times, as a steady state is eventually reached, and the optimal value of the fin porosity approaches its value in steady state operation [33]. Note that porosity values above the optima shown in Fig. 8 involve a significant drop in effective thermal conductivity, so as to negate the improvement in advective heat removal. Further, note that the sharpness in the curve shown in Fig. 8 is simply because before a certain time period, it is not optimal for the fin to be porous at all, which has been indicated by a zero value for ϕ_{opt} in the curve.

The results presented in this sub-section are of much practical importance in the design of the porous fin for transient heat removal. These results indicate that the choice of how porous the fin is designed to be depends critically, among other factors, on the time period available for heat removal. For short-time heat removal processes, making the fin porous is not helpful at all, as fin porosity worsens thermal conductivity, which directly impacts conductive heat removal that dominates at early times. This loss may

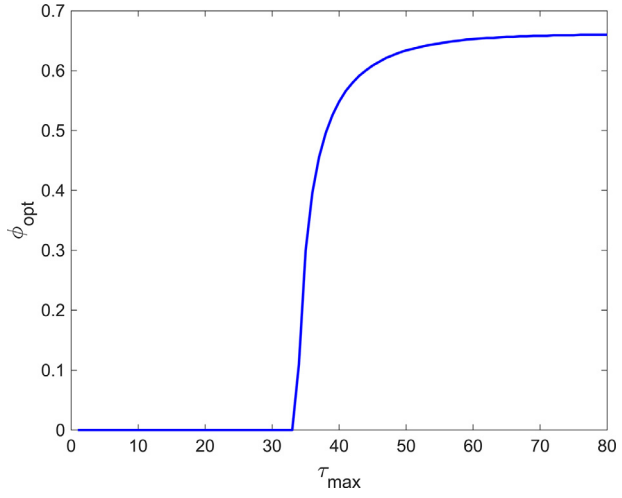

Fig. 8. Impact of porosity: Optimal porosity to maximize total heat removal as a function of total time available for heat transfer. Problem parameter are the same as Fig. 6.

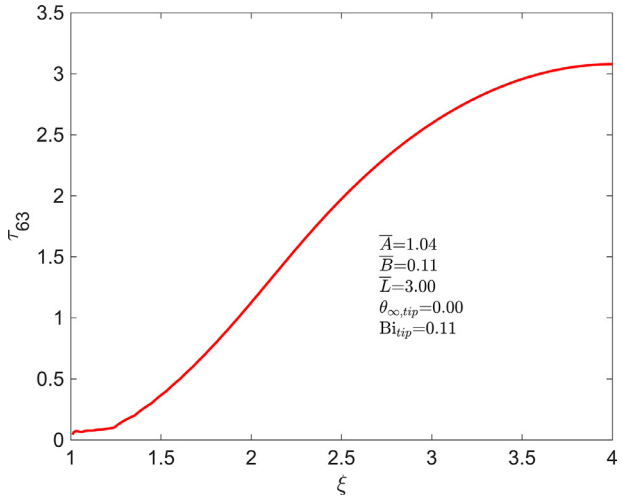

Fig. 9. Time required for 63.2% of the temperature change as a function of location along the fin. Parameter values are $\bar{A} = 1.04$, $\bar{B} = 0.11$, $\bar{L} = 3.0$, $Bi_{tip} = 0.11$, $\theta_{\infty,tip} = 0.00$.

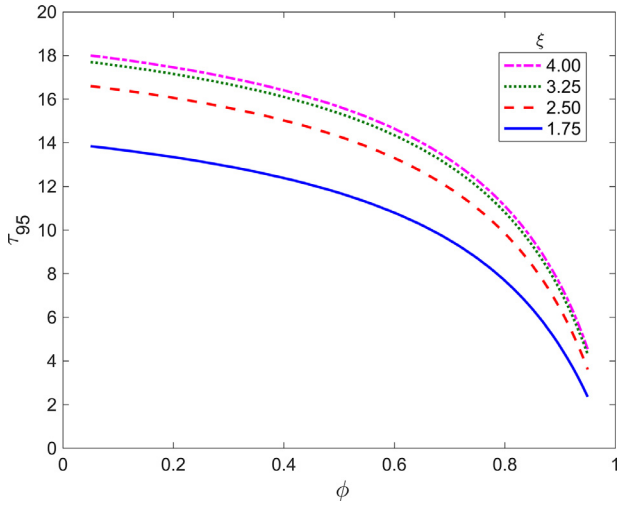

Fig. 10. Time required for 95% of the temperature change as a function of porosity at three different fin locations. Parameter values are $\bar{L} = 3.0$, $\theta_{\infty,tip} = 0.0$.

not be justified by the additional advective heat removal due to the porous flow when the heat removal time period is short.

5.6. Time taken to reach steady state

The time taken to reach steady state is an important performance parameter of interest in transient thermal systems. In the context of a porous fin, this is important to determine in order to ascertain if previously reported steady state characteristics of the porous fin [33] can be used within the time frame of interest. If the operating time of the porous fin is shorter than the characteristic time to steady state, then the transient analysis presented here must be accounted for.

Plots of the total heat removal rate from the fin as a function of time are already presented in Fig. 6, from where, the time taken to reach steady state may be estimated. For example, from Fig. 6(a), it may be inferred that the instantaneous rate of heat removal reaches within 5% of the eventual steady state value by around $\tau = 5.0$.

A more quantitative representation of time to steady state may be carried out in terms of the transient temperature distribution. Since the initial temperature is known, but the temperature field reaches steady state, in principle, only asymptotically at infinite time, therefore, the time taken to achieve, say, 95% of the temperature change may be used to represent the time taken to reach steady state. Alternately, one may use the classical definition of the thermal time constant of a lumped thermal mass, defined as the time to reach $(1 - 1/e)$, i.e., 63.2% of the temperature change. These quantities are denoted by τ_{95} and τ_{63}, respectively.

Fig. 9 plots the time taken to reach 63.2% of the temperature change as a function of spatial location on the fin. Problem parameters are $\bar{A} = 1.0$, $\bar{B} = 2.0$, $\bar{L} = 3.0$, $Bi_{tip} = 0.5$, $\theta_{\infty,tip} = 0.0$. Note that since the fin is not a lumped thermal mass, therefore, different locations on the fin reach steady state at different rates. Fig. 8 shows that fin locations close to the fin base reach steady state very quickly, as expected, due to the physical proximity to the fin base that is responsible for temperature rise. τ_{63} then rises rapidly before reaching a plateau as one approaches the tip of the fin. This is mainly because once far enough from the fin base, the time taken to reach steady state is no longer a strong function of distance from the fin base but instead is influenced more strongly by thermal conditions at the fin tip.

The time taken to reach steady state is also expected to be a function of fin porosity, because the fin porosity influences the rates of conductive and advective heat removals, which eventually contribute towards reaching steady state. Fig. 10 plots τ_{95}, the time taken for 95% of the temperature change as a function of fin porosity. It is found that at each location on the fin, τ_{95} reduces with increasing porosity, slowly at first at small porosities, and more rapidly when the porosity is larger. Note, however, that at extremely large porosity, the fin may become perforated, thereby invalidating some of the assumptions made in this work. Moreover, a highly porous fin may be structurally weak. This must be considered carefully in determining the best value of fin porosity for a particular problem.

5.7. Effect of tip conditions

Finally, the effect of fin tip conditions on heat removal rate is examined in Fig. 11. The two fin tip parameters of relevance are the fin tip Biot number, Bi_{tip}, representative of the convective heat transfer coefficient at the fin tip, and the fin tip temperature $\theta_{\infty,tip}$. Heat removal rate is plotted as a function of time for different values of these parameters in Figs. 11(a) and (b), respectively, for a representative set of parameter values. Specifically, the fin length is taken to be $\bar{L} = 0.5$. Fig. 11(a) shows that at early times, the heat removal rate does not depend on the Biot number at the tip. This is mainly because at small times, the thermal wave has not reached the tip, and, therefore, the convective heat transfer coefficient at the tip is not yet influential on the heat removal rate. At larger times, the greater the tip Biot number, the greater is the heat removal rate, as expected, due to increased heat removal from the fin tip. In each case, a steady state for the heat removal rate is reached. A large value of Bi_{tip} results in reaching steady state somewhat faster.

Similar to Bi_{tip}, $\theta_{\infty,tip}$ also influences the heat removal rate. Fig. 11(b) shows greater heat removal rate for smaller values of $\theta_{\infty,tip}$, as expected, due to the cooling effect at small $\theta_{\infty,tip}$ that induces greater heat removal from the fin base. Similar to Bi_{tip}, heat removal is relatively independent of $\theta_{\infty,tip}$ at small times, and a steady state is reached at large times.

Note that the fin length is expected to play an important role in determining how influential fin tip conditions are on heat removal rate from the fin base. The results presented in Fig. 11 are based on a somewhat short fin, $\bar{L} = 0.5$. Calculations for a longer fin, say, $\bar{L} = 2.0$ show that fin tip conditions continue to influence the heat

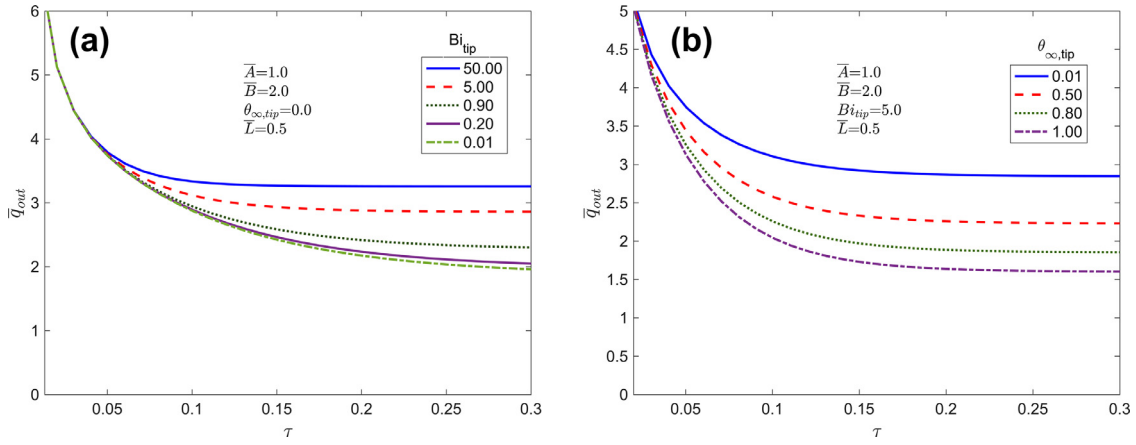

Fig. 11. Effect of fin tip conditions: (a) Heat lost through the fin as a function of time for different Bi_{tip}. (b) Heat lost through the fin as a function of time for different $\theta_{\infty,tip}$. Parameter values are $\bar{A} = 1.0$, $\bar{B} = 2.0$, $\bar{L} = 2.0$. In part (a), $\theta_{\infty,tip} = 0.0$ and in part (b), $Bi_{tip} = 5.0$.

removal rate, but not as strongly as the $\bar{L} = 0.5$ case presented in Fig. 11.

6. Conclusions

The key contribution of the present work is to develop an analytical model for transient performance of a porous fin with radially outwards pressure gradient driven porous flow. Advective heat removal due to such porous flow supplements conductive heat removal. However, the two heat removal mechanisms are influenced differently by key properties of the porous fin, and, therefore, a detailed analysis of transient temperature distribution and the resulting heat removal rate from the fin base is necessary. The analytical solution of the transient CDR equation involving Bessel functions makes it possible to identify important non-dimensional parameters and quantitatively understand their impact on fin performance.

While the steady state performance of such a porous fin has been presented recently, this work addresses the important aspect of transient performance, which may be relevant in a number of practical scenarios, such as battery thermal management, in which, heat removal occurs only for a short, transient period. In such cases, previously available steady state results are not directly applicable. One interesting result of practical relevance is that the optimal porosity that maximizes heat removal rate depends on the time period over which heat removal by the fin occurs. Such considerations may be important in practical problems that are inherently transient in nature.

Declaration of Competing Interest

The authors declare that they have no known competing financial interests or personal relationships that could have appeared to influence the work reported in this paper.

CRediT authorship contribution statement

Muhammad M. Abbas: Formal analysis, Validation, Data curation. **Mohsen Torabi:** Conceptualization, Methodology, Writing – original draft, Writing – review & editing. **Ankur Jain:** Conceptualization, Methodology, Formal analysis, Validation, Investigation, Data curation, Project administration, Writing – original draft, Writing – review & editing.

Data availability

Data will be made available on request.

References

[1] A.D. Kraus, A.M. Aziz, J.R. Welty, Extended Surface Heat Transfer, John Wiley, New York, 2002.
[2] R.L. Webb, B. Sunden, N.H. Kim, Principles of Enhanced Heat Transfer, Routledge, Boca Raton, 2005.
[3] D. Harper, W. Brown, Mathematical Equations for Heat Conduction in the Fins of Air Cooled Engines, National Advisory Committee on Aeronautics, 1922 NACA Report 158.
[4] A. Sadeghianjahromi, C.C. Wang, Heat transfer enhancement in fin-and-tube heat exchangers – a review on different mechanisms, Renew. Sustain. Energy Rev. 137 (2021) 110470, doi:10.1016/j.rser.2020.110470.
[5] R.J. McGlen, R. Jachuck, S. Lin, Integrated thermal management techniques for high power electronic devices, Appl. Therm. Eng. 24 (2004) 1143–1156, doi:10.1016/j.applthermaleng.2003.12.029.
[6] A. Mostafavi, M. Parhizi, A. Jain, Theoretical modeling and optimization of fin-based enhancement of heat transfer into a phase change material, Int. J. Heat Mass Transf. 145 (2019) 118698:1–10, doi:10.1016/j.ijheatmasstransfer.2019.118698.
[7] T. Ambreen, M.H. Kim, Effect of fin shape on the thermal performance of nanofluid-cooled micro pin-fin heat sinks, Int. J. Heat Mass Transf. 126 (2018) 245–256, doi:10.1016/j.ijheatmasstransfer.2018.05.164.
[8] G. Fabbri, Heat transfer optimization in internally finned tubes under laminar flow conditions, Int. J. Heat Mass Transf. 41 (1998) 1243–1253, doi:10.1016/S0017-9310(97)00209-3.
[9] A. Mostafavi, A. Jain, Thermal management effectiveness and efficiency of a fin surrounded by a phase change material (PCM), Int. J. Heat Mass Transf. 191 (2022) 122630, doi:10.1016/j.ijheatmasstransfer.2022.122630.
[10] A. Bejan, Entropy generation minimization: the new thermodynamics of finite-size devices and finite-time processes, J. Appl. Phys. 79 (1996) 1191, doi:10.1063/1.362674.
[11] N. Sahiti, F. Krasniqi, X. Fejzullahu, J. Bunjaku, A. Muriqi, Entropy generation minimization of a double-pipe pin fin heat exchanger, Appl. Therm. Eng. 28 (2008) 2337–2344, doi:10.1016/j.applthermaleng.2008.01.026.
[12] A. Bejan, M. Almogbel, Constructal T-shaped fins, Int. J. Heat Mass Transf. 43 (2000) 2101–2115, doi:10.1016/S0017-9310(99)00283-5.
[13] X. Liu, Y. Huang, X. Zhang, C. Zhang, B. Zhou, Investigation on charging enhancement of a latent thermal energy storage device with uneven tree-like fins, Appl. Thermal Eng. 179 (2020) 115749, doi:10.1016/j.applthermaleng.2020.115749.
[14] D. Dannelley, J. Baker, Natural convection heat transfer from fractal-like fins, J. Thermophys. Heat Transf. 27 (2013) 692–699, doi:10.2514/1.T4100.
[15] C. Yu, X. Zhang, X. Chen, C. Zhang, Y. Chen, Melting performance enhancement of a latent heat storage unit using gradient fins, Int. J. Heat Mass Transf. 150 (2020) 119330, doi:10.1016/j.ijheatmasstransfer.2020.119330.
[16] B.S. Mekki, J. Langer, S. Lynch, Genetic algorithm based topology optimization of heat exchanger fins used in aerospace applications, Int. J. Heat Mass Transf. 170 (2021) 121002, doi:10.1016/j.ijheatmasstransfer.2021.121002.
[17] M. Turkyilmazoglu, Exact heat-transfer solutions to radial fins of general profile, J. Thermophys. Heat Transf. 30 (2015) 1–5, doi:10.2514/1.T4555.
[18] W. Khan, A. Aziz, Transient heat transfer in a functionally graded convecting longitudinal fin, Heat Mass Transf. 48 (2012) 1745–1753, doi:10.1007/s00231-012-1020-z.
[19] B. Kundu, K.S. Lee, Analytical tools for calculating the maximum heat transfer of annular stepped fins with internal heat generation and radiation effects, Energy 76 (2014) 733–748, doi:10.1016/j.energy.2014.08.071.
[20] S. Kiwan, M.A. Al-Nimr, Using porous fins for heat transfer enhancement, ASME J. Heat Mass Transf. 123 (2001) 79–795, doi:10.1115/1.1371922.

[21] M. Torabi, H. Yaghoobi, Series solution for convective-radiative porous fin using differential transformation method, J. Porous Media 16 (2013) 341–349, doi:10.1615/JPorMedia.v16.i4.60.
[22] S.H. Park, J.H. Jeong, Analytical fin efficiency model for open-cell porous metal fins based on Kelvin cell assumption, Int. J. Heat Mass Transf. 196 (2022) 123283, doi:10.1016/j.ijheatmasstransfer.2022.123283.
[23] S. Kiwan, Thermal analysis of natural convection porous fins, Transp Porous Media 67 (2007) 17–29, doi:10.1007/s11242-006-0010-3.
[24] R. Das, Forward and inverse solutions of a conductive, convective and radiative cylindrical porous fin, Energy Conv. Manag. 87 (2014) 96–106, doi:10.1016/j.enconman.2014.06.096.
[25] T. Zhao, H. Tian, L. Shi, T. Chen, X. Ma, M. Atik, G. Shu, Numerical analysis of flow characteristics and heat transfer of high-temperature exhaust gas through porous fins, Appl. Therm. Eng. 165 (2020) 114612, doi:10.1016/j.applthermaleng.2019.114612.
[26] B. Buonomo, F. Cascetta, O. Manca, M.A. Sheremet, Heat transfer analysis of rectangular porous fins in local thermal non-equilibrium model, Appl. Thermal Eng. 195 (2021) 117237, doi:10.1016/j.applthermaleng.2021.117237.
[27] A. Keyhani, S. Hossainpour, M.M. Rashidi, M.A. Sheremet, Z. Yang, Comprehensive investigation of solid and porous fins influence on natural convection in an inclined rectangular enclosure, Int. J. Heat Mass Transf. 133 (2019) 729–744, doi:10.1016/j.ijheatmasstransfer.2018.12.156.
[28] L. Khoa, I. Pop, M.A. Sheremet, Numerical simulation of solid and porous fins' impact on heat transfer performance in a differentially heated chamber, Mathematics 10 (2022) 263, doi:10.3390/math10020263.
[29] A. Moradi, T. Hayat, A. Alsaedi, Convection-radiation thermal analysis of triangular porous fins with temperature-dependent thermal conductivity by DTM, Energy Convers. Manag. 77 (2014) 70–77, doi:10.1016/j.enconman.2013.09.016.
[30] J. Ma, Y. Sun, B. Li, H. Chen, Spectral collocation method for radiative–conductive porous fin with temperature dependent properties, Energy Convers. Manag. 111 (2016) 279–288, doi:10.1016/j.enconman.2015.12.054.
[31] M. Hatami, A. Hasanpour, D.D. Ganji, Heat transfer study through porous fins (Si_3N_4 and Al) with temperature-dependent heat generation, Energy Conv. Manag. 74 (2013) 9–16, doi:10.1016/j.enconman.2013.04.034.
[32] B. Kundu, D. Bhanja, K.S. Lee, A model on the basis of analytics for computing maximum heat transfer in porous fins, Int. J. Refrig. 55 (2012) 7611–7622, doi:10.1016/j.ijheatmasstransfer.2012.07.069.
[33] A. Jain, M. Abbas, M. Torabi, Steady state thermal analysis of a porous fin with radially outwards fluid flow, Int. J. Heat Mass Transf. 209 (2023) 124109:1–12, doi:10.1016/j.ijheatmasstransfer.2023.124109.
[34] J. Mathew, S. Krishnan, A review on transient thermal management of electronic devices, J. Electron. Packag. 144 (2022) 010801, doi:10.1115/1.4050002.
[35] D.W. Hahn, M.N. Özışık, N.J. Hoboken, Heat Conduction, 3rd ed., Wiley, 2012 ISBN: 9780470902936.
[36] W.M. Kays, M.E. Crawford, B. Weigand, Convective Heat and Mass Transfer, McGraw-Hill Higher Education, Boston, 2005 ISBN: 9780071238298.
[37] M. Kaviany, Principles of Heat Transfer in Porous Media, 2nd Ed., Springer, New York, NY, 1995, doi:10.1007/978-1-4612-4254-3.
[38] A. Jain, S. McGinty, G. Pontrelli, L. Zhou, Theoretical modeling of endovascular drug delivery into a multilayer arterial wall from a drug-coated balloon, Int. J. Heat Mass Transf. 187 (2022) 122572:1–17, doi:10.1016/j.ijheatmasstransfer.2022.122572.
[39] E.B. Nauman, Chemical Reaction Design, Optimization and Scaleup, 2nd Ed, John, Wiley & Sons, Hoboken, NJ, 2008 ISBN: 9780470282069.
[40] E. Augeraud-Véron, C. Choquet, É. Comte, Optimal control for a groundwater pollution ruled by a convection–diffusion–reaction problem, J. Optimiz. Theory & Appl. 173 (2017) 941–966, doi:10.1007/s10957-016-1017-8.
[41] M. Abramowitz, I. Stegun, Handbook of Mathematical Functions, United States Department of Commerce National Bureau of Standards, 1964.
[42] A. Jain, M. Parhizi, L. Zhou, Multilayer one-dimensional convection-diffusion-reaction (CDR) problem: analytical solution and imaginary eigenvalue analysis, Int. J. Heat Mass Transfer 177 (2021) 121465:1–11, doi:10.1016/j.ijheatmasstransfer.2021.121465.